5-1973

1972 Progress Report: Soil as a Factor in Modelling the Phosphorus Cycle in the Desert Ecosystem

J. J. Jurinak
Utah State University

R. A. Griffin
Utah State University

1972 PROGRESS REPORT

SOIL AS A FACTOR IN MODELLING THE PHOSPHORUS CYCLE IN THE DESERT ECOSYSTEM

J. J. Jurinak, Project Leader

and

R. A. Griffin

Utah State University

Research Memorandum, RM 73-46

MAY 1973

Report Volume 3

Page 2.3.5.6.

ABSTRACT

The research conducted in 1972 emphasized a nutrient assay of soil from the Curlew Valley site, phosphorus inventory of the vegetation and rabbit droppings, and further chemical characterization of soil phosphorus, which also included determination of the kinetics and energetics of the calcium carbonate-phosphate system.

Nutrient assay of the Curlew Valley soil included measurement of the growth responses of corn and crested wheatgrass to additions of N, P and micro-nutrients. The effect of the soil crust on growth was also assessed. The results indicated that the maximum N and P levels of 200 and 80 kg/ha of N and P, respectively, increased biomass production 500% over the check treatment. As little as 50 and 20 kg/ha of N and P, respectively, increased biomass production 367% over the check.

Polynomial relationships were generated from the yield data to predict biomass production of crested wheatgrass from the phosphorus soil test values for the condition when adequate N is added to the soil and also for when no N is added to the soil. The data also showed that crested wheatgrass gave a 67% greater growth response to phosphorus than corn when no nitrogen was added to the soil. It was concluded that, by addition of phosphorus at the time of seedling, seedling vigor of crested wheatgrass could be improved, thereby increasing the probability of success when establishing new stands.

The long-term nutrient supplying capacity of the soil was determined by harvesting the crested wheatgrass at six-week intervals. The results of the third harvest showed that the N, P, and micro-nutrient treatments yielded 2,043% more biomass per pot than the check. The rate of P uptake by crested wheatgrass during the 24-week growth period was found to vary between 10.6 µg P/day/pot found in the check treatment and 44.2 µg P/day/pot found at the maximum N and P levels.

A phosphorus inventory of five plant species and the droppings of rabbits and cows was tabulated. The phosphorus content of crested wheatgrass was found to vary between 175 ppm for the dead grass in February to 1550 ppm for the viable grass in May. It was estimated that less than 3% of the above ground phosphorus is cycled in rabbit droppings.

For ease in thermodynamic modelling, a study was conducted that modified a previously derived relationship between ionic strength, which is used in the calculation of activity coefficients of ionic species, and the electrical conductivities of natural aqueous systems. The new relationship incorporated a correction for possible ion-pair formation. The relation found was:

$$I \simeq .013\ EC \qquad r = .996$$

where I is the ionic strength, and EC is in millimhos/cm at 25 C. This relationship allows the ionic strength of a solution to be determined without chemically analyzing the system.

The kinetics and energetics of the calcium carbonate-phosphate system were studied. The rate constants and thermodynamic parameters for both the adsorption and desorption are tabulated and discussed.

INTRODUCTION

The goal of this project is to gain insight into the role of phosphorus in the production of vegetative biomass in a cold desert ecosystem. Soil phosphorus is important because of its relationship to the nutrition of native vegetation. Plant nutrient availability is a major ecological factor in determining plant biomass production and distribution. To provide the information needed to evaluate the cycling of phosphorus in the ecosystem, the intensity, capacity, and kinetic factors which regulate the movement and distribution of soil phosphorus in the profile are being studied. An inventory of the phosphorus content of the major plant species and rabbit droppings found at the Curlew Valley site was also undertaken. An inventory of the amount of phosphorus cycled by the above-ground system is vital to prediction of phosphorus flow in the phosphorus cycle submodel.

Research conducted in 1971 was primarily directed toward the chemical characterization of the soils of the Curlew Valley site. The distribution, form and movement of phosphorus in the soil received particular attention. The 1972 research stressed plant nutrient availability in soils as an ecological factor in determining plant biomass production; the chemical characterization of phosphorus also received attention. The intensity, capacity, distribution, and form of soil phosphorus was determined in 1971. However, the rate of indigenous phosphorus release in the soil and the effect of added phosphorus on the rate and amount of plant growth were still needed to complete the model. The 1971 results showed that the form of soil phosphorus was predominately calcium phosphates. It was found that the previous year's results could be refined and improved by correction for the formation of ion-pairs. Since the vast majority of soil phosphorus was the calcium phosphate mineral complex, the logical extension of the chemical characterization was the determination of the mechanism and rate of the adsorption-desorption process for the calcium carbonate-calcium phosphate mineral system. The results of the rate expressions obtained from the laboratory prediction of phosphorus release were compared with the rate of phosphorus uptake by crested wheatgrasses determined in the fertility response experiments. The results are interpreted in terms of the postulated mechanism for phosphorus interaction with calcium carbonate. These data will be vital in the modelling of the phosphorus cycle and in the ultimate modelling of biomass production and distribution among the vegetative constituents, and the flow of energy and matter within the ecosystem.

OBJECTIVES

The objectives of the research conducted in 1972 were:

1. To investigate the general fertility status of the soil at the Curlew Valley site with emphasis on the relation between the phosphorus content and the biomass production.
2. To determine the potential capacity of the Curlew Valley soil to sustain plant biomass production when natural nutrient cycling was interrupted by the action of man.
3. To inventory the phosphorus content of natural vegetation, litter and animal residues at the Curlew Valley site.
4. To continue the chemical characterization of phosphorus in the soils of the Curlew Valley site. Specifically, to determine the mechanism and kinetic rate constants for the phosphorus flux between the solution and the calcium phosphate mineral system which is dominant in the Curlew Valley soils.

The objectives accomplished in 1972 differ from those given in the original proposal in that field plots to assess the growth responses and species distribution changes of the native vegetation under field conditions were not conducted. The elimination of the field trials was the result of a reduction in the project funding.

METHODS

Fertility experiments

Soil for the fertility experiments was sampled from the surface 46 cm in March of 1972 at a site just north of hectare 6 of the crested wheatgrass site at Curlew Valley. The natural vegetation around the site was representative of the sagebrush-dominated complex common to the area. Chemical characterization of the soil was essentially identical to that described in the 1971 progress report (RM 72-38) and in the results section of this report (DSCODE A3UJD01 and A3UJD02).

The soil was sieved through a 6 mm screen and two kg aliquots were weighed into white plastic pots. Nitrogen was added in the form of ammonium nitrate solution at the rate of 50, 100 and 200 kg/ha. Phosphorus was added in the form of phosphoric acid at the rate of 20, 40 and 80 kg/ha. Potassium was added in the form of potassium sulfate solution at the rate of 100 kg/ha. Micronutrients were added together in solution as: Cupric sulfate, 20 kg/ha; zinc sulfate, 50 kg/ha; ammonium molybdate, 1kg/ha; sequestrine 330 iron chelate, 10 kg/ha; and sequestrine manganese chelate, 10 kg/ha.

The seed used was *Agropyron desertorum*, var. Nordan, foundation seed from the 1970 harvest of the Crops Research Division, No. Great Plains Research Center, Box 459, Mandan, North Dakota, 58554; and *Zea mays*, var. Iochief.

The experimental design was 3 replications of an incomplete factorial in N and P with comparisons with potassium, micronutrients, and soil crust additions. Further detail is given in DSCODE A3UJD05. In addition, 3 replications of each phosphorus treatment, including crust additions, were incubated moist in the lab to determine phosphorus soil test values at each fertilizer level when no extraction by a crop occurred.

Phosphorus soil test values are determined as ppm of 0.5 M sodium bicarbonate soluble phosphorus. Plant tissue phosphorus content was determined by perchloric acid digestion. Phosphorus content of solutions was determined by the ascorbic acid method of Murphy and Riley (1962).

Long-term phosphorus and micronutrient supplying ability of the soil was determined by repeated harvesting of the crested wheatgrass. The grass was clipped 2 cm above the soil surface and dried in paper bags at room temperature. The dry weight of the tops was measured. Phosphorus content of the tops was determined and an 8 mm plug of soil was taken and analyzed for phosphorus content after each harvest. Nitrogen was added as needed while all other nutrients were supplied in the initial treatments.

The fertility experiments were conducted in a growth chamber where light conditions were maintained at a 16 hr day and 8 hr night. Temperature was maintained at 25 C during the light period and 12 C during the dark period. Relative humidity was not controlled but was observed to be approximately 40% a majority of the time.

Phosphorus inventory

The phosphorus content inventory of vegetation of five plants and droppings of two animal species was accomplished by random sampling at four different times of the year. The rabbit droppings, however, were collected from a randomly selected square meter in both the crested wheatgrass and sagebrush communities; dried, weighed and analyzed for phosphorus content. Further detail is available in DSCODE A3UJD03.

Chemical studies

Saturation paste extracts were prepared from soil samples collected from hectares 6 and 42 of the crested wheatgrass plot and hectare 39 of the sagebrush plot of the Curlew Valley site. Nine samples were taken at each site to depths up to 165 cm. The chemical analytical data for approximately 124 river waters used in this study were picked at random from two sources (Geological Survey Water Supply Paper, 1969; Thorne and Thorne, 1951).

Electrical conductivity was determined with a Beckman Model RC-19 conductivity bridge using a 2-ml pipette cell (G1) with a cell constant of 1.00. The concentrations of the

following ions were determined by standard methods (Black, 1965; Perkin-Elmer, 1971): Ca^{++}, Mg^{++}, Na^{+}, K^{+}, HCO_3^{-}, $CO_3^{=}$, $SO_4^{=}$, Cl^{-}, phosphorus, and boron.

The measured ionic concentrations were corrected for ion-pair-formation to "actual" ionic concentrations using the method described by Adams (1971). The dissociation constants used for the ion-pair calculations were obtained from Garrels and Christ (1965). The activity coefficients for the ion pairs were assumed to be unity. The analytical data were corrected in the various experiments for the following ion pairs: $CaSO_4^{\circ}$, $CaCO_3^{\circ}$, $CaHCO_3^{+}$, $MgHCO_3^{+}$, $NaSO_4^{-}$, KSO_4^{-}, $MgCO_3^{\circ}$, $CaHPO_4^{\circ}$, $CaH_2PO_4^{+}$, and $CaOH^{+}$.

Calcium ion activity was measured with an Orion liquid ion exchange specific ion electrode coupled to an expanded scale pH meter and a calomel reference electrode. "Electrode" activity coefficients were determined from the ratio of calcium activity measured by the electrode and the "actual" or ion-pair corrected calcium ion concentration (Adams, 1971).

The sorption of phosphate was studied by shaking aqueous suspensions of calcium carbonate in solutions containing variable amounts of K_2HPO_4. X-ray diffraction studies showed the crystalline form of the calcium carbonate to be calcite. The surface area of the calcite and soil was measured by the ethylene glycol retention method of Bower and Gschwend (1952).

In order to examine the crystal surface, samples of the phosphated and pure calcite were sent to the Department of Anatomy, University of California, Davis, where electron micrographs of platinized replicas were taken.

The suspensions of calcium carbonate were shaken in a thermostated water bath which maintained the temperature at $\pm$ 0.5 C. After the suspensions were shaken, the calcuim carbonate was separated by means of a Millipore microfiber glass filter. Aliquots taken for phosphate sorbed were calculated from the difference between initial and final phosphate concentration.

Solubility criteria for the existence of calcium phosphate minerals were determined by the method of Clark and Peech (1955) which was modified to include the octocalcium phosphate solubility expression reported by Lindsey and Moreno (1960) and corrected for ion pairs. It should be pointed out that, in the construction of the solubility diagram, a range of Ksp values for hydroxylapatite can be chosen. Values given by Wier, Chien and Black (1971) vary between 109.2 and 120.2. The value of 111.8 as given by Farr (1950) and used by Clark and Peech (1955) in their original construction of the calcium phosphate solubility diagram, was used in this study. Ionic strength was determined from the electrical conductivity of the solution by the method of Griffin and Jurinak (1973).

Equilibrium studies were conducted by shaking suspensions of 4.00 gm of calcite placed in 125 ml Erlenmyer flasks with a 50 ml volume of phosphate solution and equilibrated at various temperatures. The initial phosphorus concentrations ranged from 0.1 to 5.0 ppm. The tops of the flasks were covered with parafilm in which a small hole was made to allow equilibration with atmospheric carbon dioxide. The flasks were shaken for periods of 2 to 3 days at a given constant temperature. The pH was assumed constant due to the buffering ability of the calcite-carbon dioxide system.

Interpretation of the equilibrium adsorption data was aided by application of the familiar Langmuir (1918) and B.E.T. (Brunauer, Emmett and Teller, 1938) equations. Obtaining adsorption data at different temperatures allowed the differential isosteric heat of adsorption $\overline{\Delta H}$, to be determined by application of the Clausius-Clapeyron equation (Klotz, 1964).

Long term adsorption kinetic studies were carried out as described in the equilibrium studies except that flasks were removed from the water bath and filtered after periods of time varying from a few minutes up to two months. Reaction time in all cases is defined as the period between when solution was added until completion of filtration. Filtration time was approximately 10 sec.

Short-term kinetic studies were carried out by weighing 50 gm of calcite into a 2 liter Erlenmyer. One liter of distilled water was added and the flask shaken in a water bath. The pH was adjusted by manipulation of the carbon dioxide partial pressure in the flask until a constant value of 8.4 was reached. Fifty ml of 4.0 ppm phosphorus solution was then added and the flask vigorously stirred. At the appropriate time intervals, approximately 50 ml of the slurry was poured out onto a filter and an aliquot taken for phosphorus analysis.

Desorption kinetics were studied by weighing 5.00 gm samples of calcite into 250 ml Erlenmyer flasks. A 50 ml volume of distilled water was added to the flask and the flask shaken in a thermostated water bath for one day to allow equilibration with atmospheric carbon dioxide. To each flask was added 5 ml aliquots of 2.0 ppm phosphorus solution and shaken 2-3 days. One gm of 30-50 mesh Dowex 1-X8 anion exchange resin, which had previously been soaked in a saturated calcite solution and air dried, was then added. The flasks were vigorously shaken for various lengths of time and the resin separated form the calcite slurry on a 60 mesh sieve. The resin was then placed in a funnel with No. 1 Whatman filter paper and the phosphate exchanged off the resin with 1N Na_2 SO_4 solution. The filtrate was collected in a 50 ml volumetric flask and analyzed for phosphate.

Anion exchange resin simulates a plant root which continually takes phosphate out of solution and thus maintains a steep chemical potential gradient between solid phase phosphate and solution phosphate. It was found that 92% of the phosphate added to a solution was recovered from the resin in less than two minutes.

RESULTS AND DISCUSSION

Fertility assay

The fertility assay consisted of comparing the response of corn and crested wheatgrass to application of various plant nutrients. Corn was chosen as a standard agronomic crop for comparison of response to the on-site species, crested wheatgrass. The response of both crops to N and P additions was quite dramatic and the response surface of the N and P interaction on the yield of corn and crested wheatgrass is illustrated in Figures 1 and 2 respectively. Data points of the incomplete factorial design are indicated by a solid circle and are the means of three replications. Statistical analysis by the F test, at the 5% level, is given in Table 1 and the complete raw data is recorded in Data Set A3UJD05.

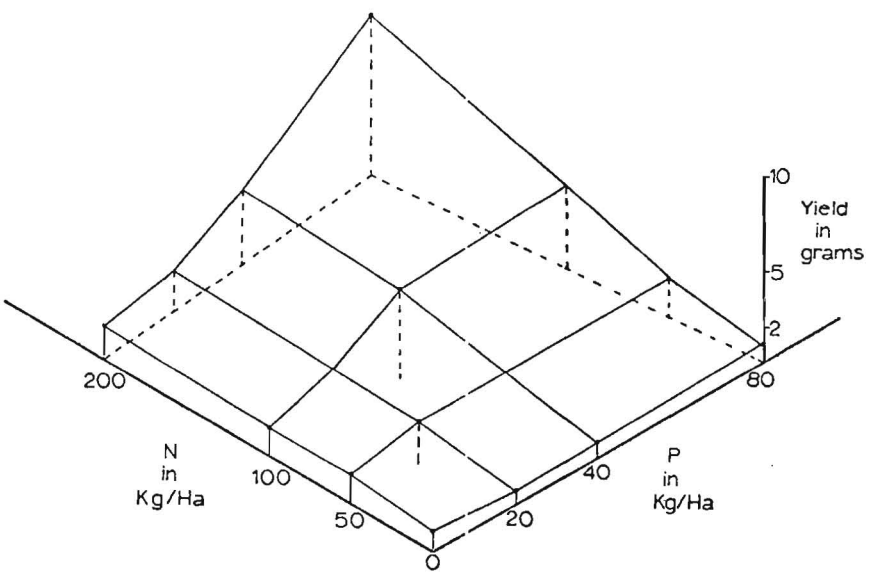

Figure 1. Response surface for corn growth showing N and P interaction. DSCODE A3UJD05

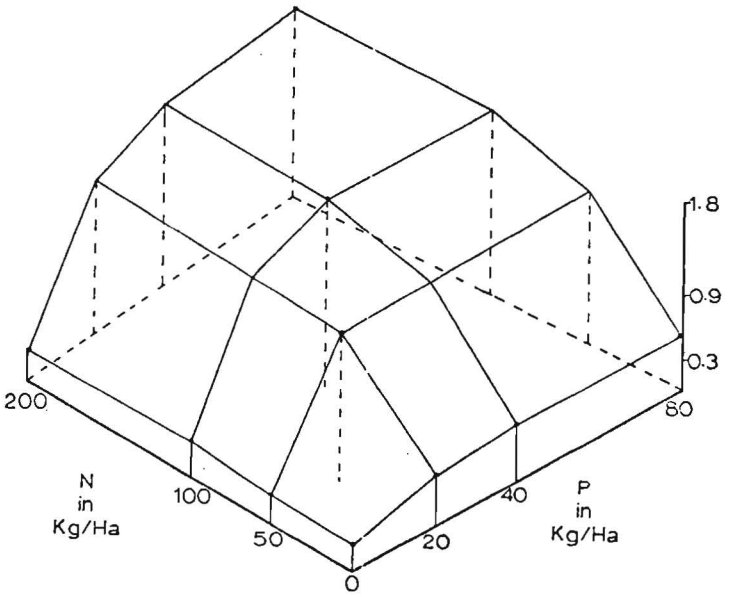

Figure 2. Response surface for crested wheatgrass growth showing N and P interaction. DSCODE A3UJD05

Table 1. Statistical analysis of N, P, and species interactions on yields of corn and crested wheatgrass. DSCODE——A3UJD05

	F 5%	Dry Wt. 1	Mg P/pot 2	Soil P ppm 3
Replications	3.74	0.25 NS	0.12 NS	2.13 NS
Species	4.60	202.5*	26.77*	0.44 NS
N	4.60	217.19*	736.03*	0.23 NS
P	4.60	143.65*	1004.75*	15.94*
SP x N	4.60	94.88*	130.91*	0.22 NS
SP x P	4.60	28.27*	148.49*	0.003 NS
N x P	4.60	125.48*	583.15*	1.01 NS
SP x N x P	4.60	33.80*	90.54*	0.62 NS

* F significant at the 5% level

The results are clear and show that the differences in yield and phosphorus uptake are significant for all interactions of plant species, N and P. Soil test values for phosphorus are all non-significant except for phosphorus fertilizer levels, which is significant. For crested wheatgrass, an N level of 200 kg/ha and a P level of 80 kg/ha gave a 500% yield increase over the check pots. As little as 50 kg/ha N and 20 kg/ha and 20 kg/ha of P gave yield increases of 367% over the check. These yield increases were greater than expected from the soil test values obtained during the 1971 research. The reason is shown in Figure 3, which gives the yield of crested wheatgrass as a function of the soil test value, i.e. ppm of sodium bicarbonate soluble P, found for the Curlew Valley soil. For standard agronomic practices, it is found that soils which give phosphorus soil test values greater than 10 ppm seldom give economical yield increases to additions of phosphorus. The results shown in Figure 3 indicate that yields did not level off when adequate nitrogen was available until phosphorus soil test values were 20 ppm P. This illustrates the desirability of individual testing of non-agronomic soils and plants when yield performance predictions are required.

The polynomial found for these experimental conditions which predicts yield (Y) for any given phosphorus soil test value (X) when adequate N is available is:

$$Y = -2.83 + .418\ X - .0091\ (X)^2 \qquad (1)$$

Similarly, the polynomial found which describes yield (Y) for a soil test value (X) when no nitrogen was added to the pots was:

$$Y = -.14 + .059\ X - .0013\ (X)^2 \qquad (2)$$

An interesting facet of these fertility experiments was the difference between corn and crested wheatgrass in their growth responses to phosphorus additions. As can be seen in Figures 1 and 2, corn made no significant increase in growth when phosphorus alone was added while crested wheatgrass growth was increased by 67% over that of the check. This difference in phosphorus response was particularly evident during the early stages of growth and is illustrated in Figures 4 and 5 for corn and crested wheatgrass respectively. Figure 4 illustrates that when only P is added to the soil, no significant differences in growth of corn, when compared to the check, can be detected. Figure 5 illustrates that the pot with P added alone has grown approximately twice as fast as either the check or with N added alone.

The most obvious application of this result is in range improvement. Crested wheatgrass seedlings have been shown to respond markedly to phosphorus additions. It is concluded that, by addition of phosphorus at the time of seeding, seedling vigor could be improved thus insuring greater success in establishing new stands of crested wheatgrass.

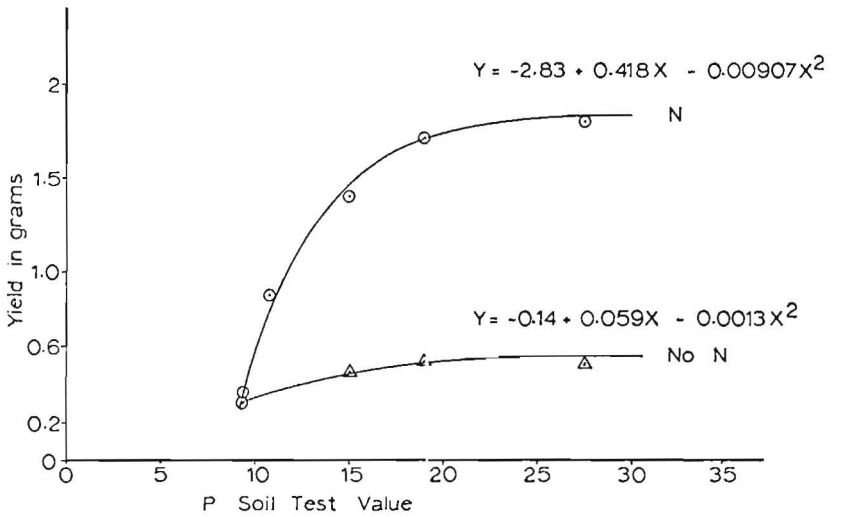

Figure 3. Relationship between phosphorus soil test value and yield of crested wheatgrass. DSCODE A3UJD05

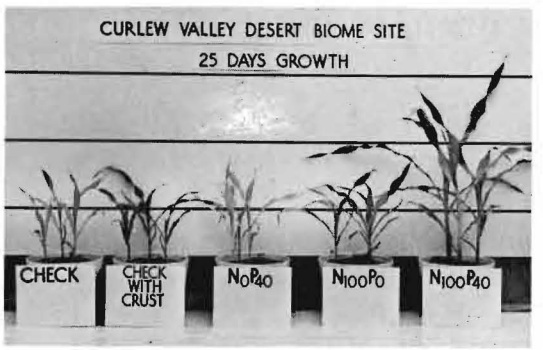

Figure 4. Growth of corn after 25 days on soil from the Curlew Valley site of the US/IBP Desert Biome.

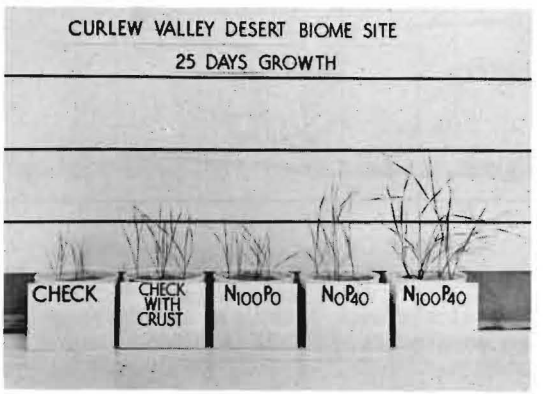

Figure 5. Growth of crested wheatgrass after 25 days on soil from the Curlew Valley site of the US/IBP Desert Biome.

Results of the 1971 research indicated that a substantial fraction of the phosphorus in the soil profile was located in the surface crust (2 cm depth). The consequence of this on the phosphorus nutrition of the plant was that even though the available P content of the crust was high (25 ppm), when diluted down with the bulk soil to 10% crust, the value was only 2.5 ppm. Therefore the addition of crust merely acted as though a small amount of P fertilizer was added to the pot with a correspondingly small increase in yield. At higher P levels the effect of the soil crust was negligible. This result is illustrated in Figures 4 and 5 for corn and crested wheatgrass respectively. The increase in growth from the crust addition is a direct response to the slight increase in the fertility level. In the field situation, the effect of the higher P content of the crust on plant nutrition is considered small.

The long-term nutrient supplying capacity of the soil under continuous cropping was determined by harvesting the crested wheatgrass at six-week intervals. The results of four harvests are shown in Figure 6.

Yields of the check fell slightly in value but remained fairly constant for all harvests.

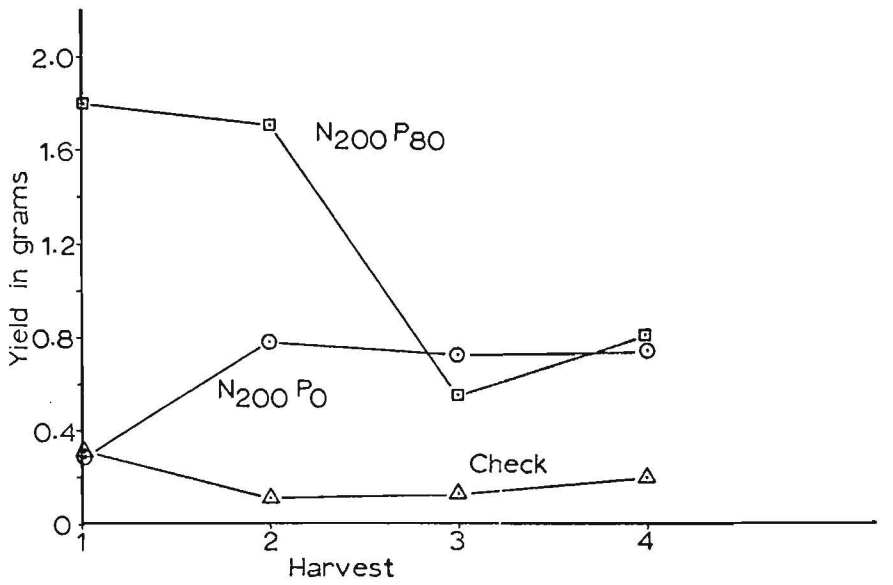

Figure 6. Effect of harvesting at six week intervals and different nutrient additions on yield of crested wheatgrass. DSCODE A3UJD05

When nitrogen alone was added, yields increased more than 50% between the first and second harvest but then remained fairly constant for the remainder of the harvests. This is presumed to be due to the development of the root system during the first harvest period and the plant being able to take advantage of it for growth during the following harvest periods. This further supports the contention that phosphorus is needed for good early growth of crested wheatgrass. Since phosphorus is known to stimulate root growth (Black, 1957), the probable mechanism is faster root proliferation.

The next significant aspect of Figure 6 is the sudden drop in yields between the second and third harvest when adequate levels of N and P were available for plant growth. The answer to this is shown in Figure 7. Treatments with micronutrients added at the start of the experiment yielded 391% more dry matter per pot than the same fertilizer level but without micronutrients added. It is speculated that the continued withdrawal of nutrients had depleted the soil of micronutrients by the end of the second harvest of crested wheatgrass.

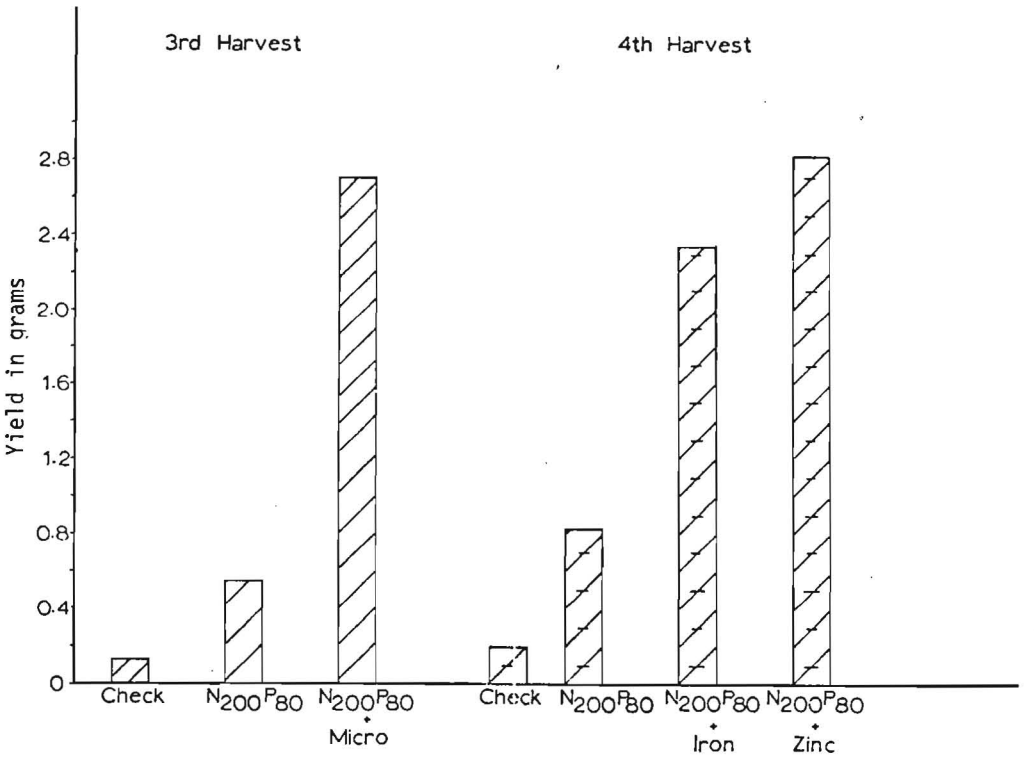

Figure 7. Effect of different nutrient additions on the yield of the third and fourth harvest of crested wheatgrass. DSCODE A3UDJ05

Iron and zinc were considered the most likely micronutrients to be limiting growth. At the end of the third harvest, these two elements were added to one pot each and the results are also shown in Figure 7. Both iron and zinc gave large growth responses indicating both were in short supply. This result is an interesting facet of the experiments but the treatment had no replication. Further work is contemplated to determine the extent of micronutrient deficiencies at the Curlew Valley site. The effect of nutrient levels on the growth of crested wheatgrass, in the Curlew Valley soil, is further amplified by the remarkable statistic that when 200 kg/ha of N, 80 kg/ha of P, and micronutrients were added at the start of the experiment, the yield of biomass per pot for the third harvest was 2,043% greater than the check treatment.

The rate of phosphorus uptake by the plants was determined and is shown in Figure 8. The rate was found to be relatively constant after the first harvest. This was assumed to be due to a more developed root system which had expanded throughout the pot and allowed the rate of P uptake to be determined from analysis of tops only without regard to the amount present in the soil. The rate of P uptake by crested wheatgrass was found to vary between 10.6 µg P/day/pot found in the check treatment and 44.2 µg P/day/pot found at the maximum N and P levels.

Phosphorus inventory

The results of the phosphorus inventory of five plant species and the droppings of rabbits and cows is present in Table 2 and in Data Set A3UJD03. These data allow the amount of phosphorus cycled in the plants to be estimated by computation from biomass data. An interesting aspect of these data is the previous contention that a large fraction of the phosphorus would be tied up in rabbit droppings. From the data collected, it is estimated that less than 3% of the total phosphorus is cycled in rabbit droppings and the greater amount of the remaining 97% is cycled by the plants.

Figure 9 shows the seasonal variation in phosphorus content of crested wheatgrass and sagebrush. Sagebrush phosphorus contents remain relatively constant at roughly 1200 ppm throughout the year while crested wheatgrass varies in value from 175ppm for the dead grass in February to 1550 ppm for the viable grass during May. This points out the seasonal variation in species which will need to be taken in to account when modelling the flow of phosphorus in the ecosystem.

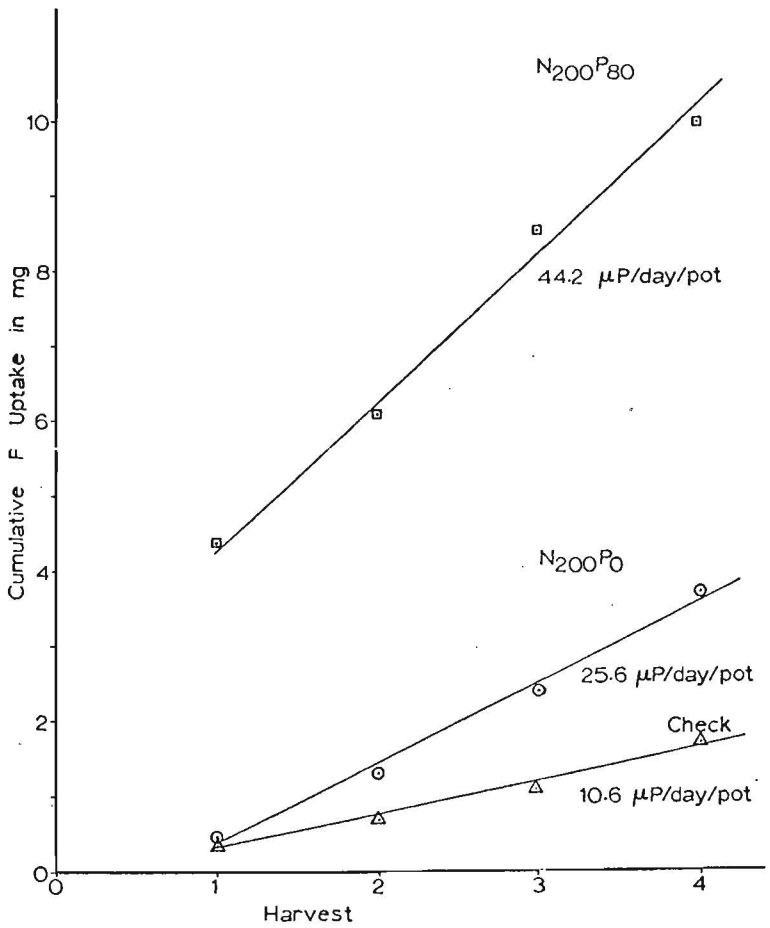

Figure 8. Effect of nutrient additions on the rate of phosphorus uptake by crested wheatgrass. DSCODE A3UJD05

Table 2. Phosphorus content of vegetation, rabbit and cow droppings collected at the Curlew Valley site of the Desert Biome DSCODE—A3UJD03

Date	Site	Hectare	Sage	Grass	Rabbit-brush	Wheat-grass	Shadscale	Litter	Rabbit Droppings	Cow Droppings
5-12-71	1	39	Tops 1462 Roots 762	Tops 1600 Roots 837	Tops 1500 Roots 737				775	
5-12-71	2	42				Tops 1550 Roots 987	Tops 887 Roots 612		3750	1275
7-13-71	1	39	Tops 1143 Roots 717	Tops 885 Roots 974	Tops 1143 Roots 735			577	1100	
7-13-71	2	42				Tops 838 Roots 935	Tops 742 Roots 1085	448	1053	
2-24-72	2	6	Tops 1338 Roots 594			Tops 175				
3-28-72	2	6	Tops 737 Roots 545			Tops 1455 Roots 635	Tops 503 Roots 460			

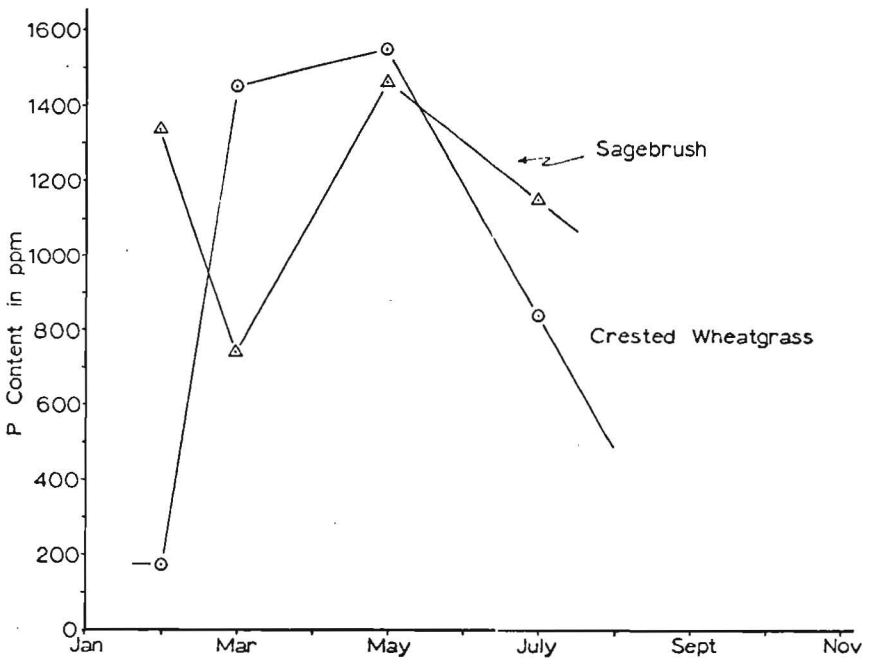

Figure 9. Seasonal variation in phosphorus content of crested wheatgrass and sagebrush. DSCODE A3UJD03

Chemical studies

The relationship between ionic strength and electrical conductivity (EC) of 27 Curlew Valley soil extracts and 124 river waters was found to be highly correlated, which corroborates the findings of Ponnamperuma,et al. (1966). The total chemical analyses of the soil extracts are given in Table 3 and Data Set A3UJD02. Figure 10 shows the observed relationship between EC and the ionic strength. The ionic strength was calculated with the analytical data corrected for ion-pair formation. The linear regression for all natural waters and soil extracts was:

$$Y = .0127\ X - .0003 \qquad r = .996 \qquad (3)$$

or

$$I \simeq .013\ EC \qquad (4)$$

where ionic strength, I, is in moles/liter and EC is in millimohs/cm at 25 C. The linear relation shown in equation (4) differs from the findings of Ponnamperuma,et al. (1966), who studied solutions considerably less saline. Correction of the computed ionic strength for ion-pair formation and extension of the data to systems of higher salinity had reduced both the slope and the scatter of data points around the regression line. These data modify the findings reported in the 1971 progress report (RM 72-38).

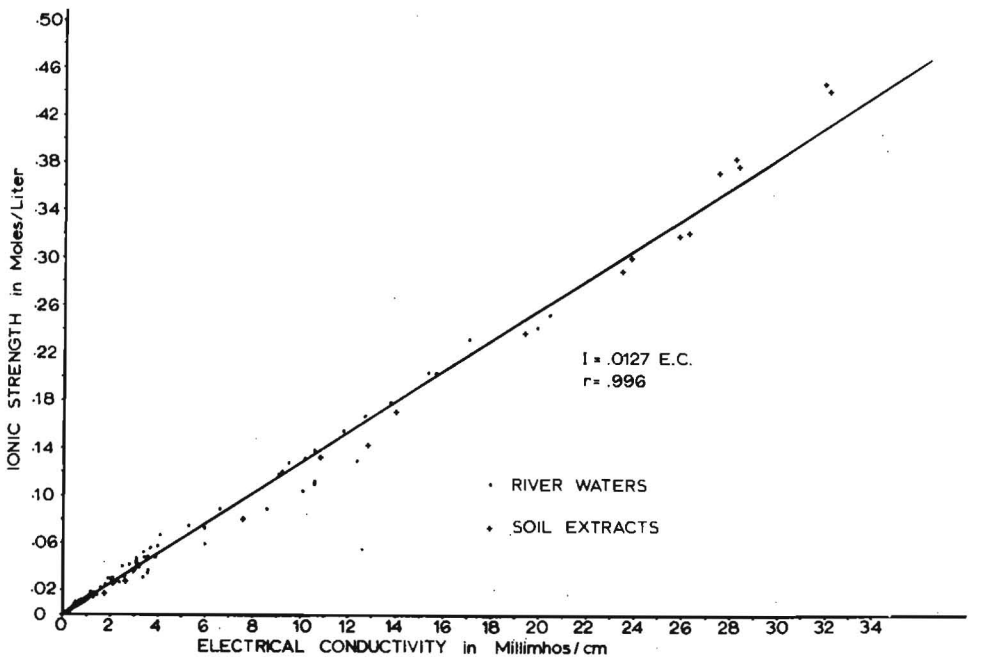

Figure 10. Relationship between ionic strength and electrical conductance of natural aqueous solutions. DSCODE A3UJD02

In the Desert Biome work, the ionic strength was used in the formulation of the thermodynamic model for the calcium-phosphate mineral complex. However, the most widely used application of the ionic strength concept is in the calculation of the mean activity coefficient of an electrolyte in solution or the individual ion activity coefficient. To verify equation (4) experimentally, the individual Ca^{+2} ion activity coefficient was determined by five methods for the 27 soil extracts whose chemical analyses are shown in Table 3. The calcium ion activity coefficient data are shown in Table 4. The "actual" individual ion activity coefficients shown in column 2, Table 4, were computed using the Davies equation and the ionic strengths shown in Table 3. These ionic strength data are computed from the total chemical analyses which were corrected for the formation of ion pairs as previously described. The "experimental" calcium ion activity coefficients shown in column 3, Table 4, were calculated from the ionic strength determined by equation (4) used in conjunction with the Davies equation. The calcium ion activity coefficient data in column 4 and 5, Table 4, were computed as above except the Debye-Hückel equation was used in the calculations. The "electrode" ion activity, as measured by the calcium specific ion electrode, and the calcium ion concentration in the extract corrected for ion pair formation.

Table 4 shows that good agreement exists between the "experimental" calcium ion activity coefficient as calculated using equation (4) and the "actual" values determined using ion-pair corrected chemical analyses with both the Debye-Hückel and Davies equations. It is interesting that more difference was noted in the values of the ionic activity coefficient computed between the two theories than between the "actual" and "experimental" values computed by each theory. This suggests that a highly accurate ionic strength value estimate is less important than selecting the proper relationship with which to compute the activity coefficient after the ionic strength value has been obtained.

The Ca^{++} ion activity coefficient values calculated from the activity of Ca^{++} obtained by the calcium specific ion electrode were consistently higher than the values obtained by the other methods. Due to the lack of complete selectivity for the calcium ion by the electrode, it appears that a great deal of confidence cannot be placed in the calcium ion activity readings from a mixed salt system e.g., soil extracts.

The data in Table 3 indicate that the lower profile samples from sites 2 and 3 were gypsiferous. Consider, for example, the 137-157 cm sample of site 2. The "actual" or ion-pair corrected calcium and sulfate concentrations were computed to be 19.55 and 26.11 mM, respectively. The activity coefficients calculated using the Debye-Hückel equation and ionic strengths computed from EC data and equation (4) were 0.26 and 0.19 for calcium and sulfate ion, respectively. Calculating the ion activity product for $(Ca^{+2})\ (SO_4^{-2})$, gives (.01955) (.26) (.02611) (.19) or 2.5×10^{-5}. The solubility product value obtained using activity coefficients computed by the Davies equation was 2.9×10^{-5}.

Table 3. Chemical analysis of saturation extracts from three profiles located at the US/IBP Great Basin Desert Biome site in Curlew Valley, Utah DSCODE——A3UJD02

Depth in cm	Concentration in mmoles/liter								Electrode Activity	Ionic Strength	E.C. mmhos cm
Site 1	Ca^{++}	Mg^{++}	Na^{+}	K^{+}	HCO_3^{-}	$CO_3^{=}$	$SO_4^{=}$	Cl^{-}	a_{Ca}^{++}		
0- 3	1.94	.42	2.21	2.49	6.12	.10	1.11	.80	1.30	12	.78
3- 13	1.72	.42	1.68	1.13	4.48	.09	1.26	.70	1.20	10	.62
13- 25	1.38	.48	2.45	1.34	3.97	.09	1.09	1.10	.90	10	.68
25- 33	.99	.38	3.24	1.78	4.10	.14	.92	1.50	.64	9	.66
33- 48	.53	.20	8.27	1.71	5.09	.13	1.53	3.00	.30	13	.91
48- 69	.30	.08	10.94	.95	7.01	.18	1.61	2.01	----	14	1.02
69- 94	.38	.26	30.15	1.45	4.43	.09	2.53	23.20	.19	35	3.02
94-137	2.46	.30	116.71	2.88	1.96	.04	3.34	116.30	.90	130	10.86
137-165	3.95	.49	150.00	3.23	1.86	.02	3.49	153.00	1.40	168	14.10
Site 2											
0- 3	2.26	.61	2.72	2.47	3.35	.23	.30	.61	1.40	10	.90
3- 15	.59	.19	3.99	1.60	2.17	.23	.37	1.20	.35	7	.64
15- 28	.49	.22	12.40	3.22	2.17	.14	.84	10.84	.30	17	1.76
28- 41	3.09	2.73	116.86	6.16	1.80	.09	6.73	116.50	1.10	141	12.92
41- 71	7.32	8.80	265.55	4.45	2.03	---	15.43	267.50	2.00	319	26.38
71- 91	5.82	8.19	275.80	3.60	1.45	---	14.64	263.75	1.70	317	25.96
91-109	18.32	13.77	279.90	4.45	.99	---	39.01	268.75	4.20	376	28.54
109-137	25.31	18.74	335.28	5.21	.67	---	43.88	307.50	5.80	446	32.16
137-157	24.74	20.76	319.89	5.21	.55	---	42.48	310.00	5.80	440	32.40
Site 3											
0- 3	2.84	.52	1.89	1.04	3.44	.14	.53	1.21	1.80	10	.80
3- 15	1.13	.30	2.28	1.11	1.13	.09	.49	2.74	.84	7	.65
15- 28	1.52	.53	18.97	2.64	1.18	.09	.92	20.00	.88	27	2.72
28- 46	1.56	.77	69.93	3.79	1.62	.12	2.88	65.00	.76	79	7.58
46- 66	5.82	5.18	205.05	4.85	.99	.05	9.16	192.50	2.00	234	19.47
66- 89	7.04	7.79	260.42	4.51	.88	.05	12.02	246.25	2.30	299	24.02
89-112	6.68	6.93	246.06	4.15	.81	.05	12.20	240.00	2.20	287	23.57
112-132	22.22	14.66	267.60	5.32	.67	---	41.75	253.75	5.40	372	27.68
132-152	23.48	16.78	267.60	5.73	.67	---	41.87	267.50	5.60	384	28.39

Table 4. Comparison of calcium ion activity coefficients obtained by three different methods DSCODE——A3UJ302

Depth in cm	Davies		Debye Hückel		
	Actual	Experimental	Actual	Experimental	Electrode
	γCa^{++}	γCa^{++}	γCa^{++}	γCa^{++}	γCa^{++}
Site 1					
0- 3	.64	.66	.66	.67	.76
3- 13	.67	.69	.68	.70	.79
13- 25	.67	.67	.68	.69	.73
25- 33	.68	.67	.68	.70	.72
33- 48	.63	.64	.64	.66	.69
48- 69	.62	.63	.63	.65	---
69- 94	.50	.49	.53	.52	.59
94-137	.34	.33	.37	.37	.40
137-165	.30	.30	.35	.34	.37
Site 2					
0- 3	.67	.66	.68	.67	.68
3- 15	.70	.69	.72	.70	.70
15- 28	.59	.57	.61	.59	.69
28- 41	.32	.31	.36	.35	.40
41- 71	.26	.25	.29	.28	.31
71- 91	.26	.26	.29	.29	.33
91-109	.25	.25	.27	.27	.29
109-137	.24	.24	.26	.26	.29
137-157	.24	.24	.26	.26	.29
Site 3					
0- 3	.67	.67	.67	.67	.67
3- 15	.70	.69	.71	.70	.78
15- 28	.54	.51	.56	.53	.60
28- 46	.39	.37	.43	.41	.54
46- 66	.28	.28	.31	.31	.54
66- 89	.26	.26	.29	.29	.38
89-112	.26	.26	.29	.29	.36
112-132	.25	.25	.27	.28	.32
132-152	.25	.25	.27	.28	.31

These data infer that the Debye-Hückel equation is superior to the Davies equation for predicting individual ion activity coefficients. This is in agreement with the view expressed by Adams (1971). However, at higher ionic strength values (> .1), the assumption was made that the activiey coefficient of the calcium sulfate ion-pair is unity (Nakajama, 1971). If this assumption is not valid, the conclusions concerning the use of these two equations may be altered.

The good agreement between the "actual" activity coefficients and those computed in conjunction with equation (4), as shown in Table 4, coupled with the ability to closely approximate the solubility product of gypsum in a gypsiferous soil, supports the validity

of equation (4). This method is considered to be sufficiently accurate for estimating the ionic strength of mixed electrolyte solutions as to eliminate the need of laborious solution and analysis of natural waters.

Another application of the derived relationship is in the prediction of EC from ionic concentration data (McNeal, et al., 1970). Theoretically, correction of analytical data for ion-pair formation and use of equation (4) should yield more reliable EC values than those obtained from regression analysis based on non-corrected concentrations or relations based on linear-segment fitting of one particular data set.

The information presented here on the interaction of phosphorus with calcite is a condensation of a more complete treatise given by Griffin (1973). The results of phosphate adsorption on calcite plotted according to the Langmuir isotherm equation are presented in Figure 11. The data show two distinct linear portions which delineate two regions of adsorption.

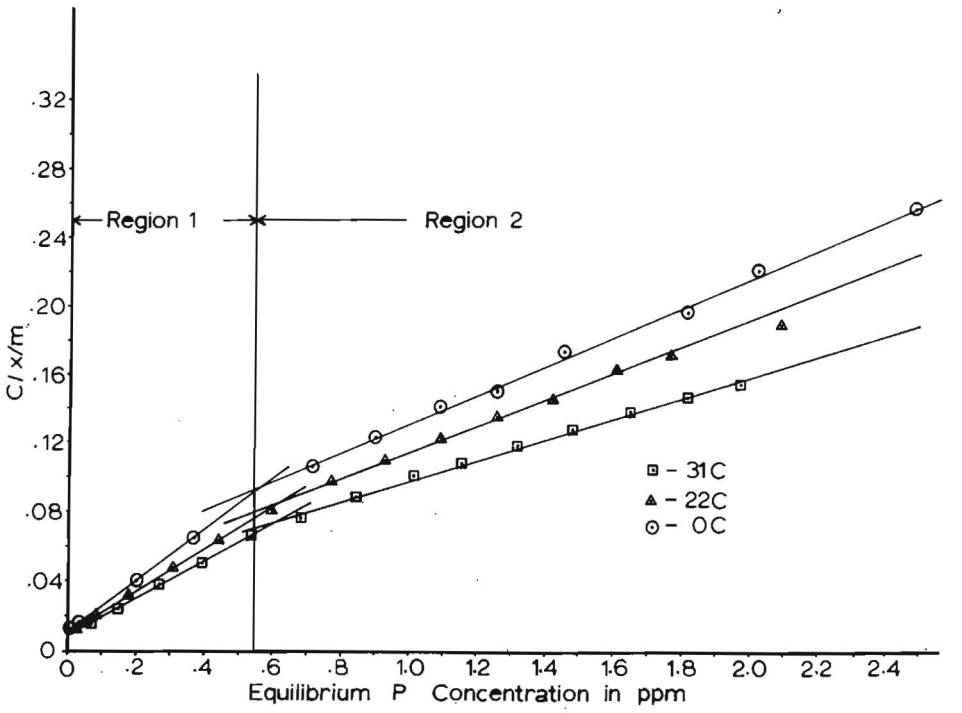

Figure 11. Phosphorus adsorption data for calcite plotted according to the Langmuir isotherm. DSCODE A3UJD02

Attempts to resolve the adsorption isotherms presented in Figure 11 into their component energy sites were unsuccessful and led to inspection of a second hypothesis, that of multilayer adsorption. The results are shown in Figure 12 and indicate that the data are linear throughout the entire applicable surface coverage range of the equation.

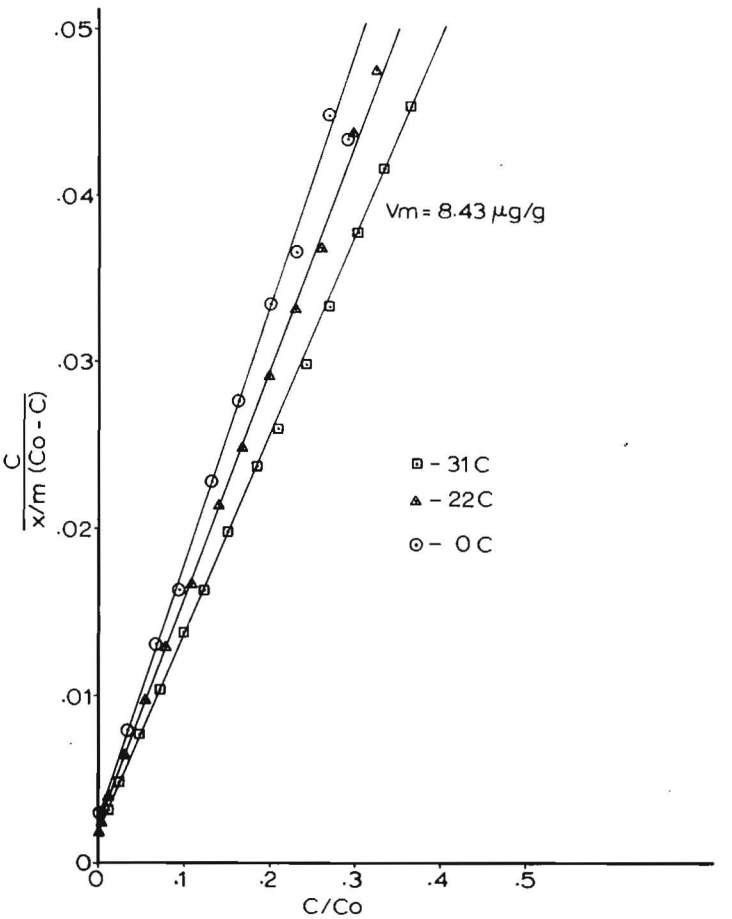

Figure 12. Phosphorus adsorption data for calcite plotted according to the B.E.T. equation. DSCODE A3UJD02

The monolayer capacity computed from the B.E.T. equation is shown in Figure 12 and agrees closely with the adsorption maximums obtained from the region 1 slopes of the Langmuir plot of Figure 11. Comparison of these monolayer capacities with the total surface area of the calcium carbonate indicate that only approximately 5% of the total surface is covered with phosphate ions. It appears that we do not have classical multilayer adsorption, but apparently have adsorption in layers at very specific sites on the surface. This leads to the hypothesis that this special kind of multilayer formation at

specific sites may be the critical cluster formation for heterogeneous nucleation of calcium phosphate on the surface of calcite.

The interpretation of heterogeneous nucleation is corroborated by electron microscope studies. Figures 13 and 14 show electron-micrographs of single calcite crystals which have been reacted with water and with phosphate solution respectively. The surface of the crystal reacted with water is relatively smooth while the crystal that has been reacted with 0.19 ppm phosphorus solution has developed surface growths which cover only a small percentage of the surface. Further support of a heterogeneous nucleation interpretation of the data presented up to this point comes from the isosteric heat of adsorption calculations.

Figure 13. Electron micrograph of platinized surface replica of unreacted calcite single crystal surfaces at 18,000 x.

Figure 14. Electron micrograph of platinized surface replica of calcite single crystal surface after reaction with phosphorus at 18,000 x.

The isosteric heat of adsorption ($\overline{\Delta H}$) gives a measure of the energy released or adsorbed during the adsorption of a molecule onto the surface. The results indicate the $\overline{\Delta H}$ is endothermic and varies between 7.73 kcal and 9.33 kcal $\pm$ 0.4 kcal and is plotted as a function of surface coverage in Figure 15. The data show that upon completion of region 1, a discontinuity in the $\overline{\Delta H}$ plot occurs which is interpreted as being due to the energy barrier created by the necessity for an internal rearrangement of the molecules on the surface. Further, after completion of a layer, the interaction energy of the surface becomes masked and the multilayer or cluster becomes less stable. This instability then allows rearrangement or nucleation and the epitaxial growth of the new calcium phosphate crystalline phase on the surface of the calcite.

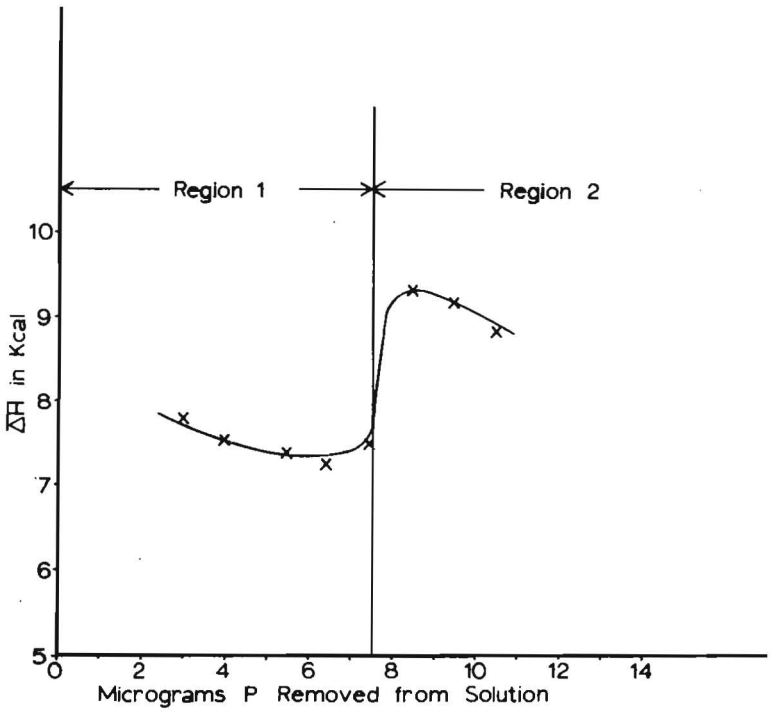

Figure 15. Isosteric differential heat of adsorption as a function of surface coverage.

To be consistent with heterogeneous nucleation theory, heats of adsorption values indicating chemisorption would be expected (Stumm and Morgan, 1970). The values for $\overline{\Delta H}$ obtained in these experiments are consistent with a chemisorption mechanism.

Using solubility criteria, region 1 and 2 can be differentiated as belonging to two different calcium phosphate mineral species. The solubility diagram for the calcium phosphates and calcium carbonate is shown in Figure 16. Selected adsorption data points are plotted on the solubility diagram. The results indicate that the calcium ion concentration is being governed by the calcite-carbon dioxide system. The results further show that the solutions in region 1 are supersaturated with respect to hydroxylapatite and that solutions from region 2 are in equilibrium with or supersaturated with respect to a second mineral species, octocalcium phosphate. These data are further support of a heterogeneous nucleation hypothesis.

Adsorption kinetics

The data obtained from long-term kinetic experiments are presented in Figure 17. The interpretation of these data are consistent with and give strong support to the heterogeneous nucleation hypothesis. The interpretations of the kinetic results provide a

summary of the interpretation given the previous data. The first important feature of the graph is the sharp initial drop in concentration which is interpreted as corresponding to the initial surface adsorption which is the precurser to the critical cluster formation. The second feature is the relatively flat portion of the graph which corresponds to the induction period prior to crystal growth. This portion is regulated by the chemical potential gradient established by the relative supersaturation of the initial solution. The higher the initial concentration, the faster the multilayer or critical cluster becomes unstable and the shorter the induction period. The third portion of the graph, where the concentration falls off to low values, may be interpreted as corresponding to the epitaxial growth of the calcium phosphate mineral species on the surface of the calcite.

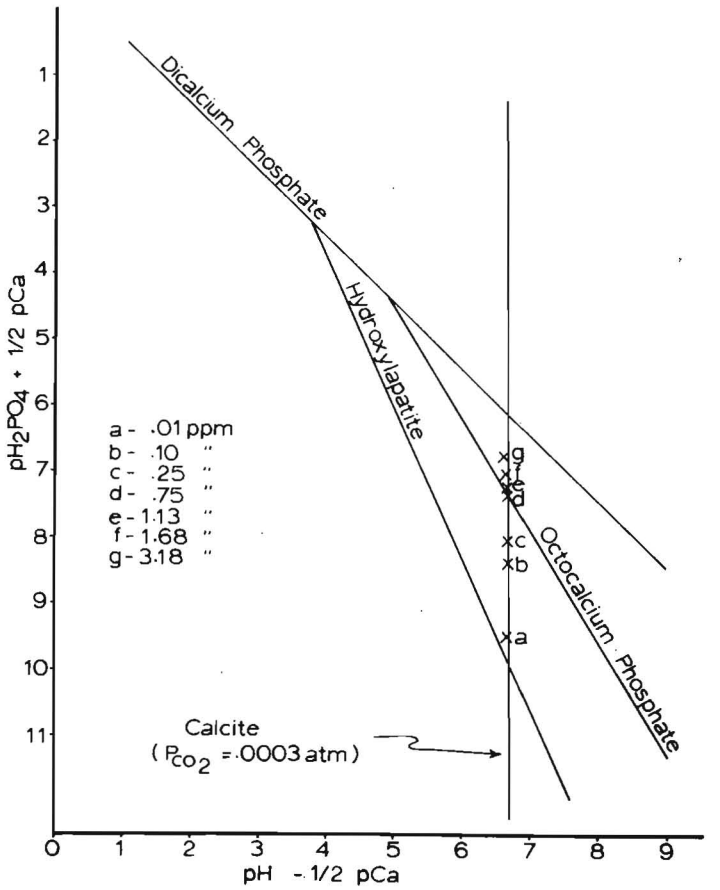

Figure 16. Solubility diagram of the calcium phosphates with selected adsorption data plotted. DSCODE A3UJD02

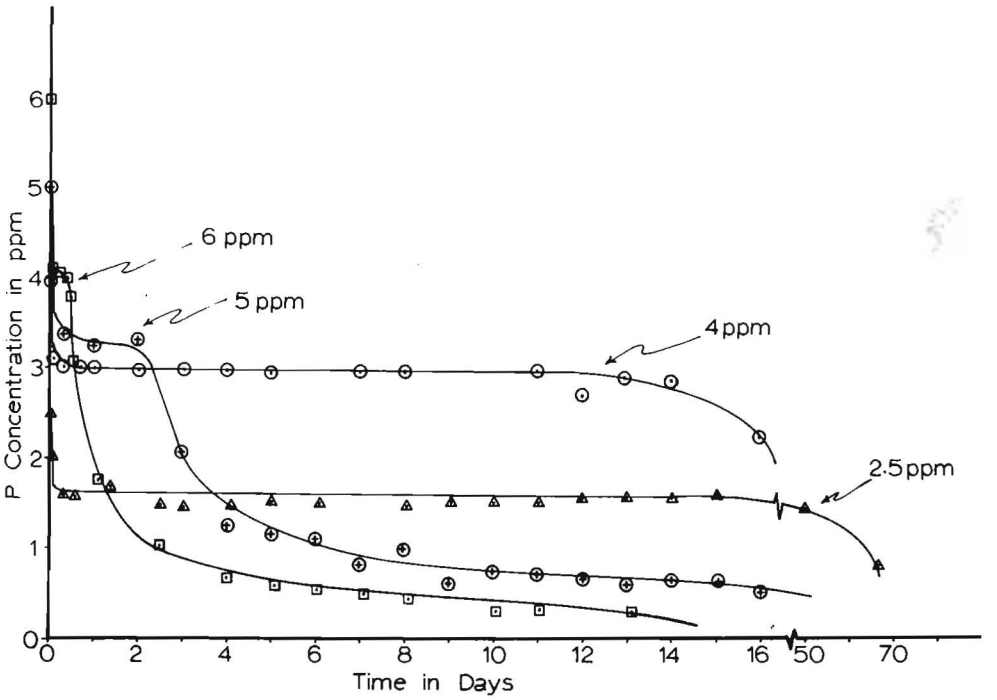

Figure 17. Long term kinetics of phosphorus interaction with calcite at 23 C and different initial phosphorus concentrations.

In order to study the initial stages of the reaction, experiments were set up to obtain data at short reaction times. It was also desired to verify if the reaction was surface-mediated or precipitation type reaction. To accomplish this later objective, an identical reaction system (see Methods section) was set up with the calcite carefully filtered out by gravity so as not to disturb the calcite-carbon dioxide equilibrium which had been established. The phosphorus was then added to the saturated solution and monitored at various times. The results of these experiments are shown in Figure 18. They indicate that the reaction is indeed surface-mediated since when no calcite was present, the concentration of phosphorus remained essentially constant during the entire four-hour reaction period. The phosphorus concentration in the samples containing calcite fell rapidly to low values within 10 to 20 min after the initiation of the reaction. If the reaction had been a precipitation of calcium phosphates, the presence of calcite should have had no influence on the reaction rate since both systems were equally supersaturated with respect to hydroxylapatite. Therefore, the conclusion was reached that the calcite surface was an important factor in the observed reaction kinetics.

The shape of the kinetic curve shown in Figure 18 made it apparent that the reaction could not be described by simple kinetic relationships. Complex reaction kinetics involving two or more simultaneous reactions were suggested by the shape of the plots.

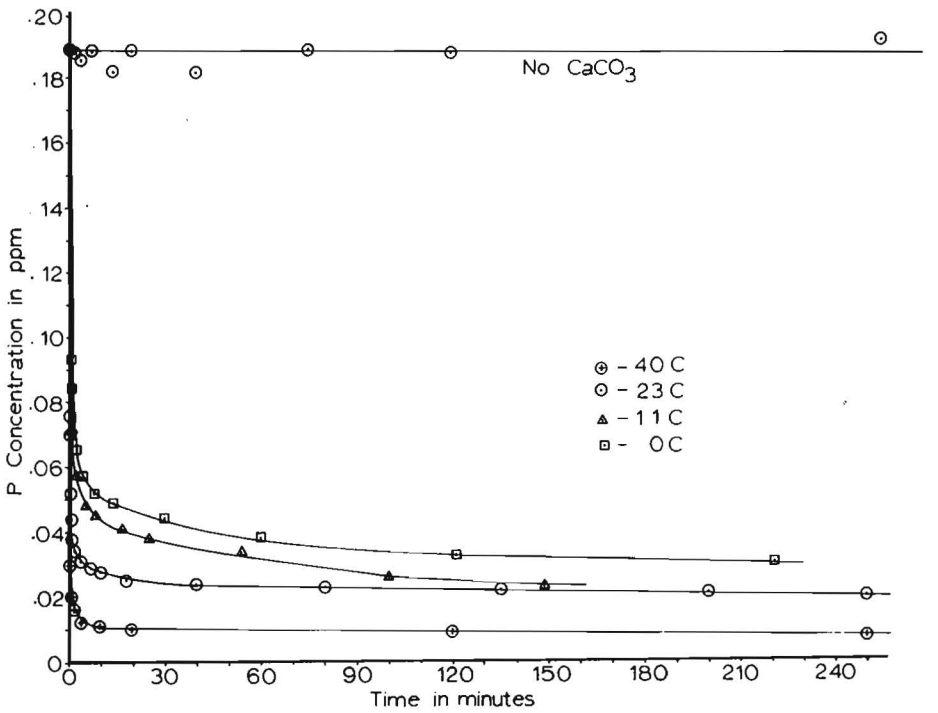

Figure 18. Kinetics of phosphorus interaction with and without calcite and at different temperatures.

The data were analyzed according to simultaneous second-order and first-order kinetics. The results are shown in Figures 19 and 20 for the first-order and second-order plots respectively. The results of these kinetic data add further support and are consistent with the postulated mechanism of a heterogeneous nucleation of calcium phosphate mineral species mediated by the surface of calcite. The postulated mechanism is the second-order adsorption of phosphorus on the surface of the calcium carbonate, that is, the rate of adsorption is regulated by the solution concentration of phosphorus and the number of empty surface sites. This is followed by a first-order reaction which is interpreted as corresponding to the surface rearrangement of the heteronuclei into the calcium phosphate crystal which supercedes crystal growth.

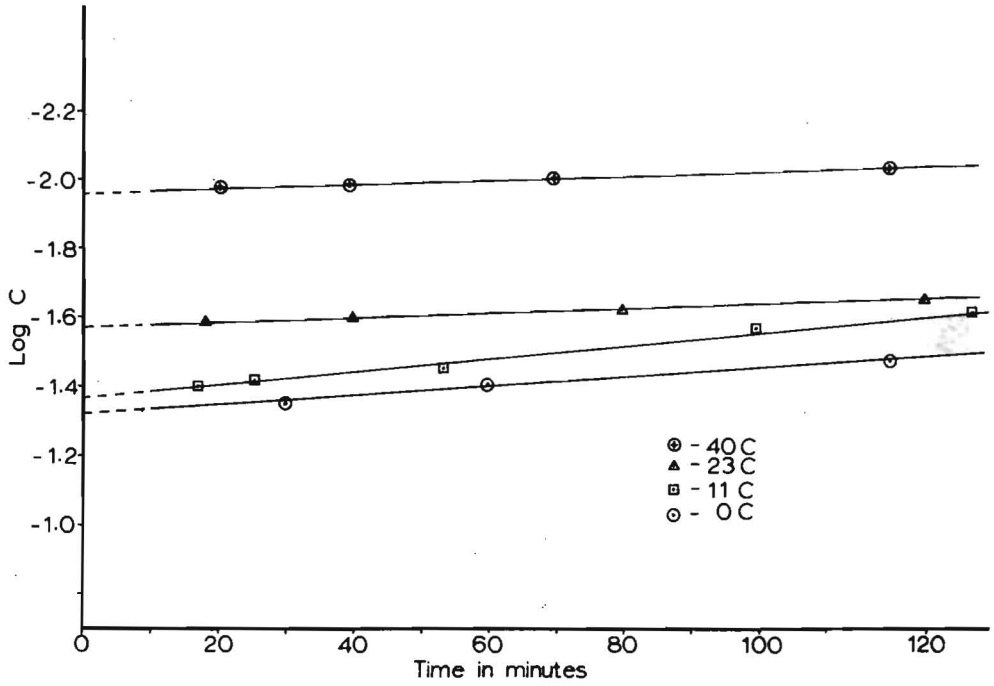

Figure 19. First-order rate plot for phosphorus interaction with calcite at reaction times greater than 10 minutes.

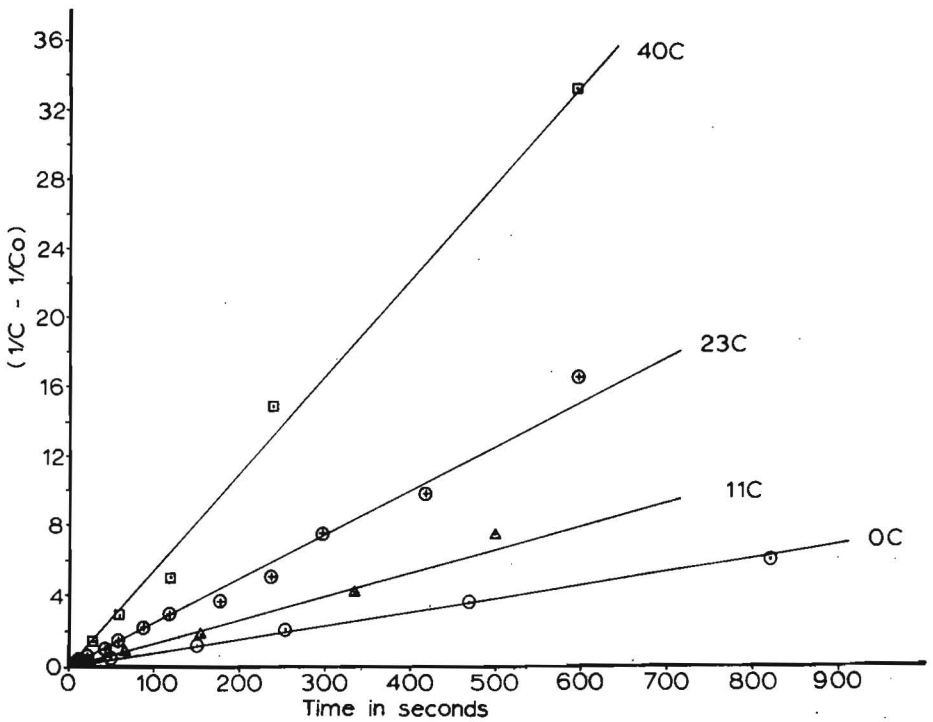

Figure 20. Second-order rate plot for initial phosphorus interaction with calcite.

The adsorption rate constants for the simultaneous reactions at various temperatures were computed from the slopes of the lines and are presented in Table 5. These rate constants were then used in the computation of activation energies, which are also given in Table 5, and will be discussed in the section on the thermodynamic parameters.

Table 5. Kinetic parameters for the adsorption and desorption process at different temperatures

	Adsorption	Nucleation	Adsorption			
Temperature in Deg. C	k_1 l/mole-sec	k_1 l/sec	Ea Kcal/mole	$\Delta H^\dagger$ Kcal/mole	$\Delta S^\dagger$ Calories deg.mole	$\Delta G^\dagger$ Kcal/mole
0	$.72 \times 10^{-2}$	$.22 \times 10^{-4}$	9.0 + 1.8	8.46	-37.2	18.62
11	$.14 \times 10^{-1}$	$.32 \times 10^{-4}$	adsorp.	8.44	-37.2	19.00
23	$.26 \times 10^{-1}$	$.10 \times 10^{-4}$	< 1 Nuc.	8.41	-37.6	19.61
40	$.55 \times 10^{-1}$	$.12 \times 10^{-4}$		8.38	-37.6	20.15
	Desorption l/sec	Dissolution l/sec	Ed	Desorption		
11		$.59 \times 10^{-4}$	1.4 ± 1 Diss			
23	$.33 \times 10^{-6}$		< 1 Desorp. 0.41		-66.0	20.1
40		$.74 \times 10^{-4}$				

To determine if the calcium phosphate mineral nucleating on the surface was the thermodynamically stable hydroxylapatite or one of the metastable calcium phosphates, some of the kinetic data (shown in Figure 18) were plotted on the calcium phosphate solubility diagram and the results are presented in Figure 21. The data for 40 C indicate that the solution reaches equilibrium with hydroxylapatite within 24 hr. At the lower temperature (11 C) the equilibrium is approached, but not reached, during the four-hour reaction time represented on the diagram. This data leads to the conclusion that the calcium phosphate mineral species nucleating on the surface is indeed hydroxylapatite. However, predicting which species will nucleate on the surface requires caution since the results of data plotted in Figure 16 indicate that the mineral species which is nucleated on the surface depends on the initial phosphorus concentration, i.e. the Ca/P ratio.

The solubility diagram gives further support to the conclusion that the relatively flat portions of the kinetic curves correspond to amorphous or semi-crystalline clusters of ions on the surface which slowly change and/or nucleate into hydroxylapatite. The rate of this crystallization or nucleation depends on the relative supersaturation of the solution to the crystal form in question. It should be noted that at low phosphate concentrations the induction period may last an indefinite period of time. This may account for

the fact that hydroxylapatite is not found in many natural systems. It is the thermodynamically stable form, but the kinetics are very slow.

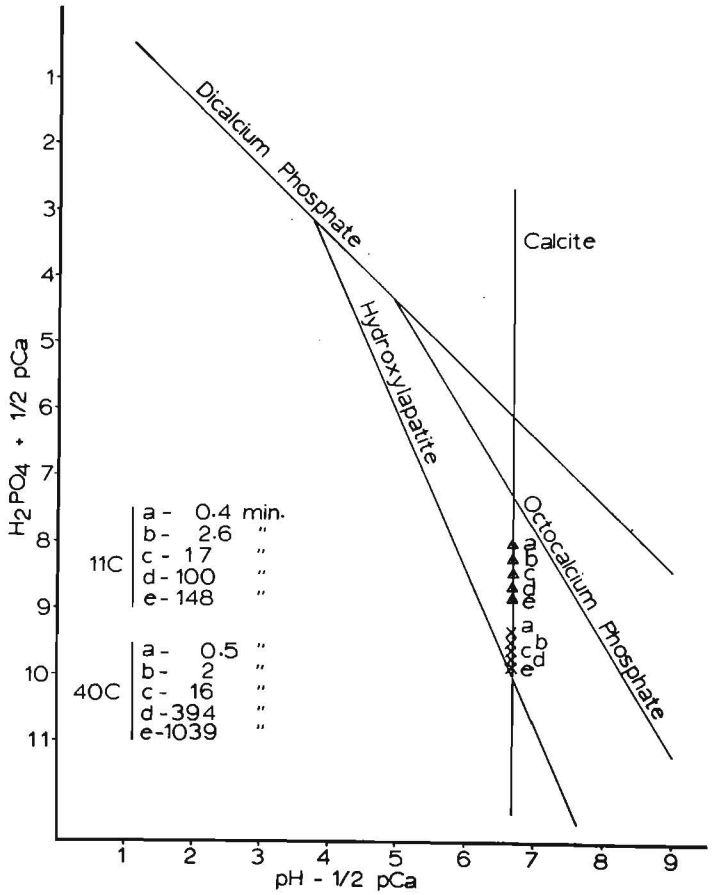

Figure 21. Solubility diagram for the calcium phosphates with kinetic data for two temperatures plotted.

Desorption kinetics

The results of desorption experiments using anion exchange resin are presented in Figure 22. The data show that between the temperatures of 11 C and 40 C there is only a small temperature dependence on the desorption of phosphorus from the calcite surface. Except for the small temperature dependence, the desorption kinetic curves are approximately the inverse of the adsorption kinetic plots. This led to the supposition that the desorption mechanism was approximately the inverse of the postulated adsorption mechanism, i.e., the desorption is the result of two simultaneous processes: that of dissolution of

the calcium phosphate mineral which was nucleated on the calcite surface and desorption of phosphate ions from the calcite surface.

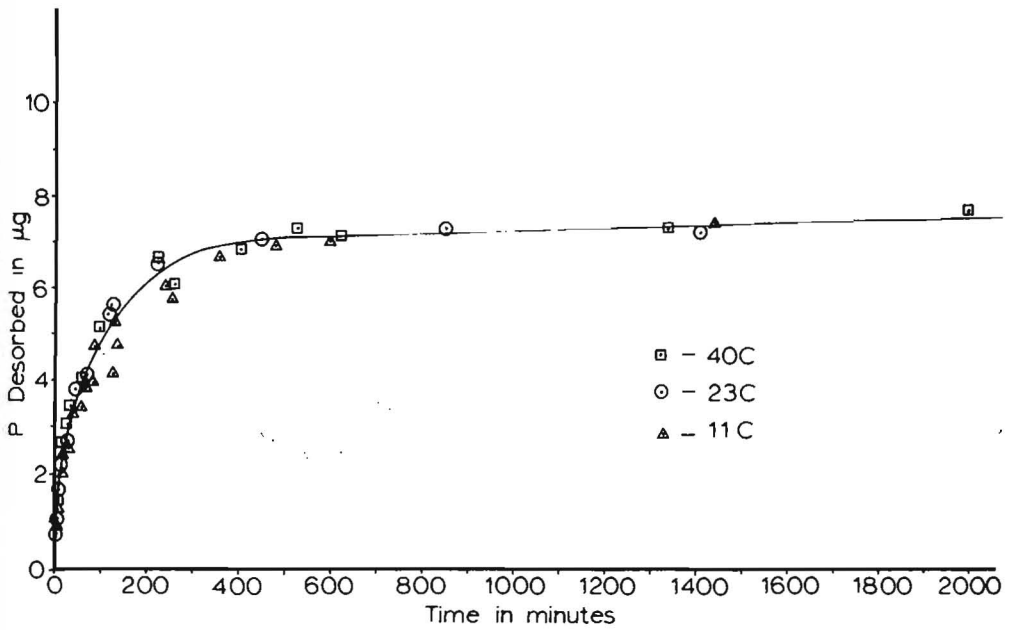

Figure 22. Kinetics of phosphorus desorption from calcite by the resin method.

To investigate the possibity that one of the mechanisms was dissolution of a mineral on the surface, the data were plotted according to the "parabolic diffusion law" given in Figure 23. The results indicate that during the initial stages of desorption (times less than 100 min) the data were found to follow the diffusion rate expression with a very slight temperature dependence.

The data for the entire 24 hr reaction period were analyzed according to simultaneous first-order reaction kinetics. The results are presented in Figure 24 and show the data to be broken into two distinct linear segments. The initial portion of the data are linear up to reaction times of 400 min. This is interpreted as corresponding to the first-order dissolution of the phosphate mineral from the surface of the calcite. The second portion of the plot also follows a first-order expression but is a much slower reaction. These data are interpreted as corresponding to a desorption of the phosphate ions from the surface of the calcite. The desorption rate constants computed from the slopes of the lines are given in Table 5.

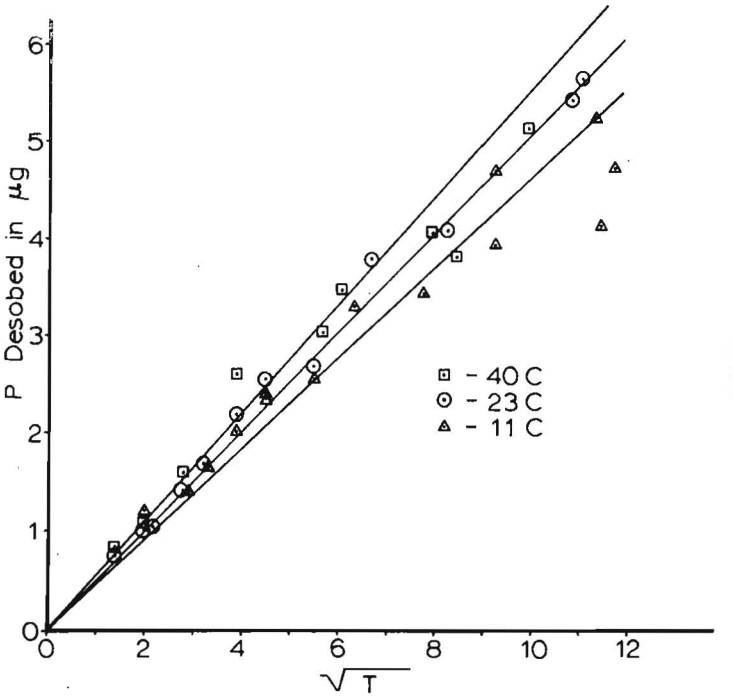

Figure 23. Phosphorus desorption data plotted according to the "parabolic diffusion law."

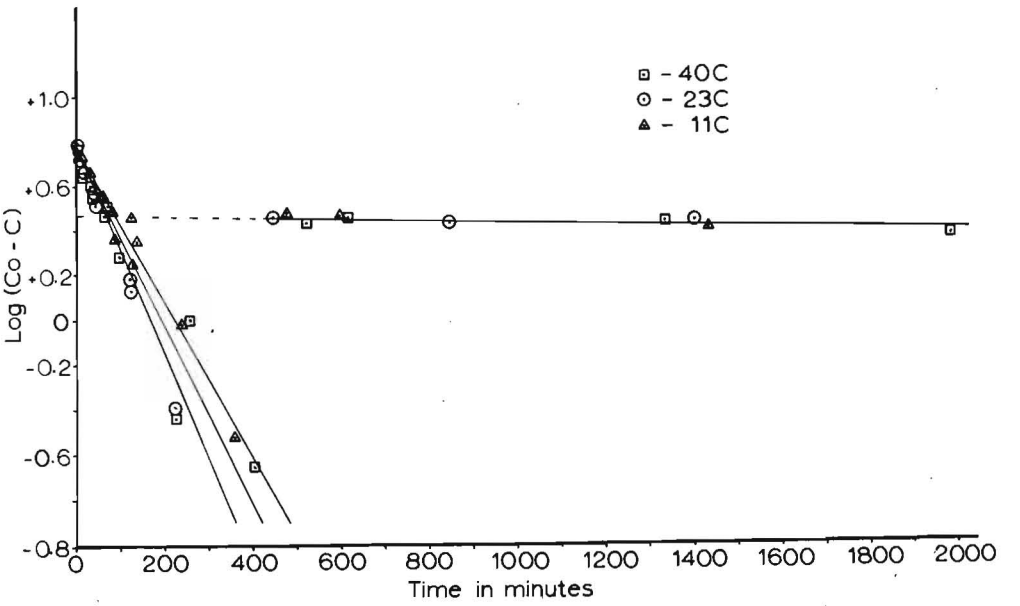

Figure 24. Phosphorus desorption data plotted according to simultaneous first-order rate expressions.

It is concluded that phosphorus desorption from calcite using anion exchange resin can be described by simultaneous first-order rate expressions. These two reaction rates are postulated to correspond to: 1. dissolution of calcium phosphate mineral nucleated on the surface with the rate-limiting step being diffusion, presumably through a static water film, and 2. desorption of phosphorus ions from the calcite surface.

Using the rate constants determined from the above study, the phosphorus desorption rate was computed to be 10.4 µg P/day/Pot. This compares to the value of 10.6 µg P/day/Pot obtained for the rate of P uptake by crested wheatgrass in the check treatment of the nutrient assay. This demonstrates that realistic rate values for phosphorus uptake by roots are estimated by resins in laboratory experiments.

Thermodynamic parameters

The activation energy of adsorption and desorption were determined from the rate constants and are given in Table 5.

The enthalpy, entropy, and free energy of activation were also computed and are given in Table 5.

Results of 1971 research pointed out that the preponderate form of soil phosphorus was the calcium-phosphate mineral complex. Now that study of the kinetics and energetics of pure calcium-phosphate mineral system is completed, study of the phosphorus flux in the more complicated soil system can proceed from a strong theoretical base.

Determination of the kinetic rate constants for the Curlew Valley soil using the concepts and techniques developed for the pure calcite system is on-going. Preliminary results using the soil indicate that the interpretation of the phosphate adsorption mechanism is nearly identical to the pure calcite system. As an example, the Langmuir adsorption isotherm for the Curlew Valley soil is given in Figure 25 and can be compared with the nearly identical-shaped isotherm shown for pure calcite in Figure 11.

The phosphorus adsorption maximum computed from Figure 25 yields a value of approximately 500 kg/ha. Experience has shown that maximum plant growth does not occur until the available phosphorus level of the soil is around 20% of the adsorption maximum. Even with 80 kg/ha of added phosphorus, this only brings the phosphorus level to 16% for the Curlew Valley soil. The effect of the percentage of the adsorption maximum on yield of crested wheatgrass is illustrated in Figure 26. This result helps explain why unusually high soil test values were required for maximum yields. This soil from the Curlew Valley site has an unusually high phosphorus adsorption capacity and bonds phosphorus more tenaciously than soils with lower adsorption capacities.

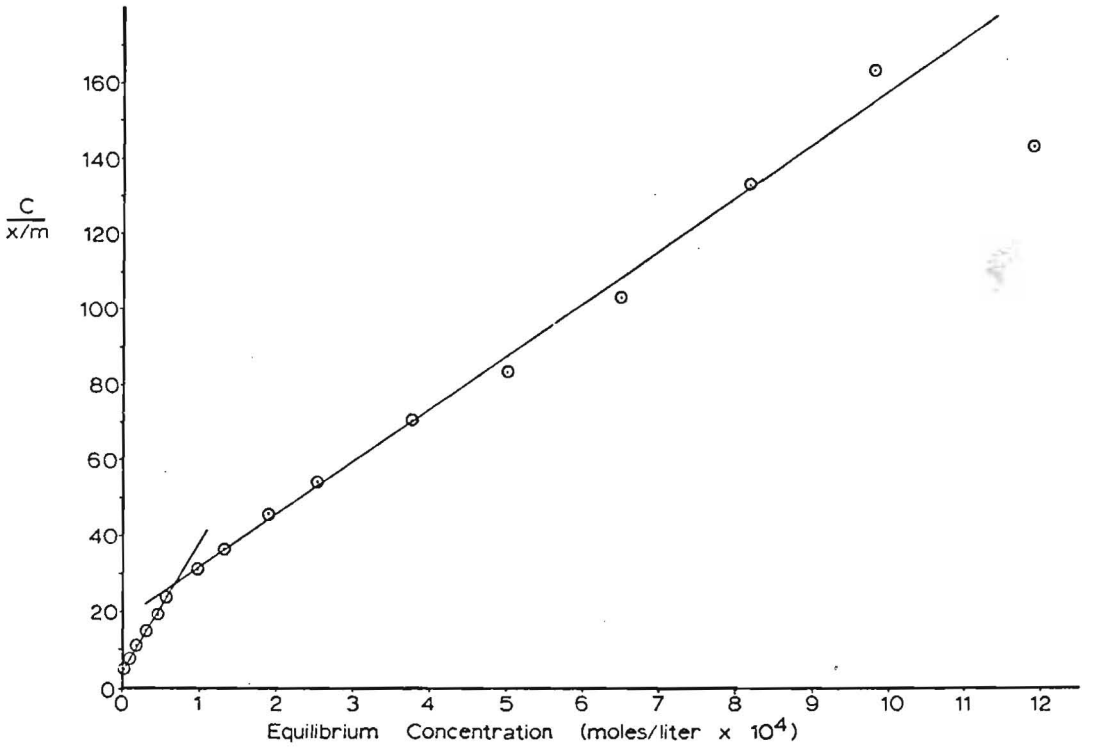

Figure 25. Phosphorus adsorption data for soil from the Curlew Valley site plotted according to the Langmuir isotherm.

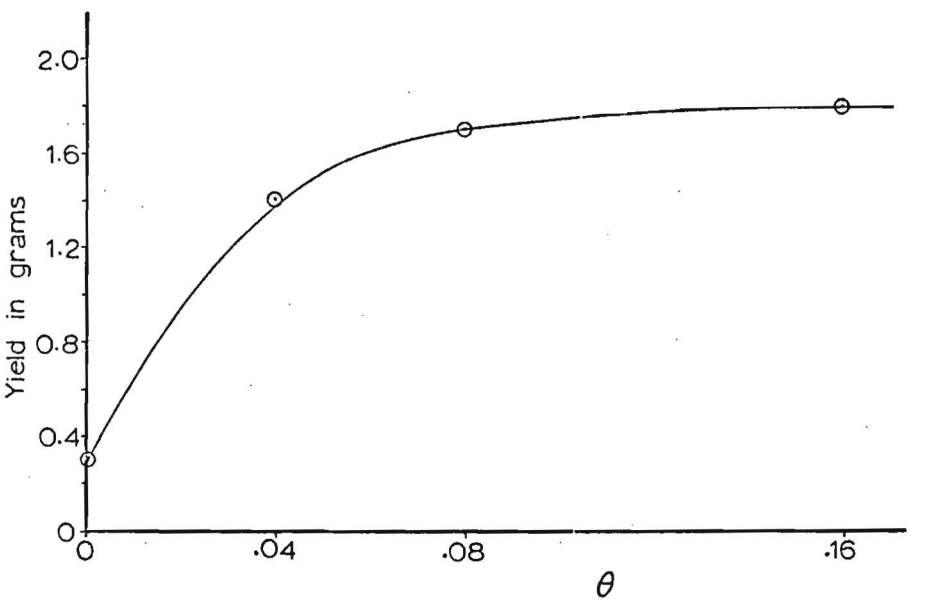

Figure 26. Yield of crested wheatgrass as a function of the percentage of the phosphorus adsorption maximum (θ) of the soil from the Curlew Valley site.

EXPECTATIONS

The research conducted during 1972 yielded data which indicated a growth response in crested wheatgrass to minor elements additions. In 1973 the growth chamber work will emphasize this aspect of plant nutrition in the soil of the Curlew Valley site of the Desert Biome. Preliminary results indicated large growth responses to both iron and zinc. The experimental design will emphasize this as an incomplete factorial of phosphorus and zinc with interlocking subsets to evaluate the added effects of zinc-iron and zinc-manganese. Nitrogen will be added at a uniform level for adequate growth as determined from the 1972 results. It is expected that in the absence of nutrient cycling, micro-nutrient deficiency will be a major factor in biomass production.

Chemical characterization of soil phosphorus will be completed in 1973 with the determination of the phosphorus flux values for the soil of the Curlew Valley site. The theory and techniques developed in 1972 enhance the possibilities for successful completion and interpretation of the soil phosphorus flux data during the 1973 project year. It is expected that the phosphorus flux rate for the soil will be similar to that obtained from the pure calcite system.

LITERATURE CITED

Adams, F. 1971. Ionic concentrations and activities in soil solutions. Soil Sci. Soc. Amer. Proc. 35:420.

Black, C. A. 1957. Soil-Plant Relationships. Wiley and Sons, New York, 322 p.

Black, C. A. (Ed.). 1965. Methods of Soil Analysis, Part 2. Agronomy Monograph No. 9, Madison, Wisconsin.

Bower, C. A., and F. B. Gschwend. 1952. Ethylene glycol retention by soils as a measure of surface area and interlayer swelling. Soil Sci. Soc. Amer. Proc. 16:342.

Brunauer, S., P. H. Emmett and E. Teller. 1938. Adsorption of gases in multimolecular layers. J. Am. Chem. Soc. 60:309.

Butler, J. N. 1964. Ionic Equilibrium, A Mathematical Approach. Addison-Wesley Co., Reading, Mass. 438 p.

Clark, J. S., and M. Peech. 1955. Solubility criteria for the existence of calcium and aluminum phosphates in soils. Soil Sci. Soc. Amer. Proc. 19:171.

Farr, T. C. 1950. Phosphorus, properties of the element and some of its compounds. Tennessee Valley Authority Chemical Engineering Report No. 8. Wilson Dam, Alabama.

Garrels, R. M., and C. H. Christ. 1965. Solutions, Minerals, and Equilibria. Harper and Row, New York. 450 p.

Geological Survey Water-Supply Paper 1967. 1969. Quality of Surface Waters for Irrigation Western States 1965. U.S. Gov. Printing Office, Washington, D.C.

Griffin, R. A. 1973. The Kinetics and Energetics of Phosphorus Interaction with Calcite. Ph.D. Dissertation, Utah State University, Logan, Utah.

Griffin, R. A., and J. J. Jurinak. 1973. Estimation of activity coefficients from the electrical conductivity of natural aquatic systems and soil extracts. Soil Sci. In Press.

Klotz, I. 1964. Introduction to Chemical Thermodynamics. Benjamin, Inc., New York. 244 p.

Langmuir, I. 1918. The adsorption of gases on plane surfaces of glass, mica, and platinum. J. Am. Chem. Soc. 40:1361.

Lindsey, W. L., and E. C. E. Moreno. 1960. Phosphate phase equilibria in soils. Soil Sci. Soc. Amer. Proc. 24:177.

McNeal, B. L., J. D. Oster, and J. T. Hatcher. 1970. Calculation of electrical conductivity from solution composition data as an aid to *in situ* estimation of soil salinity. Soil Sci. 110:405.

Murphy, J., and J. P. Riley. 1962. A modified single solution method for the determination of phosphate in natural waters. Anal. Chim. Acta 27:31.

Nakajama, F. S. 1971. Calcium complexing and the enhanced solubility of gypsum in concentrated sodium-salt solution. Soil Sci. Soc. Proc. 35:881.

Perkin-Elmer. 1971. Analytical Methods for Atomic Absorption Spectrophotometry. Perkin-Elmer Corp., Norwalk, Conn.

Ponnamperuma, F. N., E. M. Tianco, and T. A. Loy. 1966. Ionic strengths of the solutions of flooded soils and other natural aqueous solutions from specific conductance. Soil Sci. 102:408.

Stumm, W. and J. J. Morgan. 1970. Aquatic Chemistry. J. Wiley and Sons, Inc., New York. 583 p.

Tanji, K. K., and L. D. Doneen. 1966. Predictions on the solubility of gypsum in aqueous salt solutions. Water Resources Res. 2:543.

Thorne, J. P., and D. W. Thorne. 1951. Irrigation Waters of Utah. Bulletin 346, Utah State University Experiment Station, Logan, Utah.

Weir, R. R., S. H. Chien and C. A. Black. 1971. Solubility of hydroxylapatite. Soil Sci. 111:107.